Published by The College of Science & Information Technology (COSIT), TASUED, Vol. 19, No. 1, pp. 55-64.

COSIT, TASUED
Journal of Science and Information Technology (JOSIT)

A Finite Volume Method to Solve the Governing Equations of Microchannel Flow Boiling Cooling Technique

Odumosu, O.A.

Department of Industrial Technical Education, Tai Solarin University of Education
Corresponding Author: odumosuoa@tasued.edu.ng

Abstract

Microchannel flow boiling exhibits exceptional heat transfer performance, making it an ideal solution for high-heat-flux dissipation in micro-device cooling applications. Microchannel flow boiling achieves superior heat transfer by exploiting the latent heat of the working fluid and the enhanced surface-area-to-volume characteristics. This study presents a finite volume method (FVM) to numerically resolve the governing equations of microchannel flow boiling, including mass, momentum, energy, and phase-change evolution equations. The method is widely used for solving microchannel flow boiling equations due to its inherent conservation properties and ability to handle complex geometries and multiphase flows. The study provides insights into the detailed analysis of microchannel flow boiling cooling technique and enhances the fundamental understanding of multiphase flow physics required to develop the advanced cooling systems by bridging the gap between theoretical models and solution procedures.

Keywords: Microchannel, Flow boiling, Finite volume method, Phase-change heat transfer

INTRODUCTION

Flow boiling in microchannels is of considerable importance given its effectiveness in managing high heat fluxes (HHF) and excellent thermal management. Microchannel flow boiling dissipates high heat fluxes efficiently due to its high surface-area-to-volume ratio and the usage of the latent heat of the working fluid (Odumosu et al., 2023). Within a microchannel, as liquid flows through its heated channel wall, nucleation is initiated with the formation of bubbles when the liquid temperature reaches its saturated condition due to the phase-change process. A growing vapor bubble while moving downstream rapidly fills the cross-section of the microchannel. Flow boiling exploits the large latent heat required for the phase change from liquid to vapor and provides effective high heat flux cooling. The heat sinks of microchannel flow boiling are generally arranged as micro- evaporators consisting of multi-microchannels in parallel (Odumosu et al., 2024), made of highly-conductive material having direct contact with the surface to be cooled. Most common cross-sections include square, rectangular, trapezoidal, polygonal, circular, half-circular, U-shape and Gaussian beam shapes (Prakash & Kumar, 2014) as shown in Figure 1. At the inlet manifold of flow boiling microchannel heat sinks, the liquid at subcooled or saturated conditions enters the heat sink and a mixture of liquid and vapor leaves the microchannels after flowing through it (Magnini & Matar, 2020). The application areas of microchannel flow boiling include electronics cooling (Mudawar, 2013), refrigeration system, aerospace thermal management, and nuclear reactors (Karayiannis & Mahmoud, 2017; Mudawar, 2011).

The phase-change process during the flow boiling in microchannels causes changes in the bubble size and shape, and the subsequent flow regimes. Harirchian and Garimella (2012) systematically categorized microchannel flow boiling into distinct regimes - single-phase (liquid), bubbly, confined bubble (slug/plug), annular, and dry-out - with classification dependent on both heat flux and mass flux

Cite as:

Odumosu, O. A. (2024). A Finite Volume Method to Solve the Governing Equations of Microchannel Flow Boiling Cooling Technique. *Journal of Science and Information Technology (JOSIT),* Vol. 19, No. 1, pp. 55-64.

parameters. At the inception of the flow boiling in microchannels, the bubble formation occurs at the nucleation sites in the channel upstream (Harirchian & Garimella, 2012). The channel corners, surface roughness, or microstructures can behave as nucleation sites for microchannels (Al-Zaidi et al., 2019). Subsequently, after nucleation the bubbles disperse and slide along the channel wall. The bubbles continue to grow due to vaporization and coalesce with other smaller sized bubbles while moving downstream. This stage is referred to as the bubbly flow regime. As the discrete bubbles grow, they quickly expand to occupy the entire channel cross-section, transitioning into confined bubbles that evolve into elongated bubble and slug flow. In this slug flow regime, a thin liquid film separates the elongated vapor bubbles and the channel walls. The bubble train of slug flow regime in a microchannel flow boiling is shown in Figure 2. As the velocity of the vapor bubbles and liquid slugs becomes higher due to liquid vaporization and bubble expansion along the channel, the bubble shape is distorted and changed into churn flow. Further downstream, annular flow is observed with a vapor core at the center of the channel separated from the walls by a thin liquid evaporating film on the channel wall. The liquid film is typically very thin and moves along the channel wall. The slug and annular flow regimes dominate a substantial portion of the flow regime map, representing the most prevalent flow patterns in microchannels. (Revellin et al., 2006). Notably, the slug flow regime is particularly advantageous for microchannel heat exchangers, owing to its outstanding heat transfer efficiency. (Ferrari et al., 2018). The confined geometry of microchannels restricts vapor bubble growth laterally, promoting axial expansion and the formation of elongated bubbles which are surrounded by thin liquid films that enhance thermal performance (Jain & Gedupudi, 2020).

Understanding the dominant flow boiling patterns in microchannels is key to developing comprehensive tools for the design and optimization of microchannel flow boiling heat sinks (Qu et al., 2004). The flow patterns of microchannel flow boiling are affected by several factors, including the flow rate, channel geometry, surface topography, fluid properties, and operating conditions (Harirchian & Garimella, 2010, 2011; Thome & Cioncolini, 2015). The flow patterns also significantly influence the heat transfer and pressure drop in the microchannels (Saha et al., 2011).

To investigate the flow boiling heat transfer in microchannels, experiments can be performed to understand the process. A primary challenge in experimental studies lies in the insufficient spatial and temporal resolution of available instrumentation to adequately characterize micro-scale flow boiling behavior, further complicated by the intricate multi-physics nature of these processes. The difficulty of making measurements and visualization of rapid phase change phenomena at the micro-scale makes the experimental investigation very challenging. However, numerical analysis has the capability to access more complex details of the flow and heat transfer of flow boiling in microchannels. Numerical simulation via computational fluid dynamics (CFD), in addition to experiments, serves as a vital tool for comprehending the boiling in microchannels as it can offer many details that cannot be obtained experimentally. The advent of advanced computing technologies has led to the development of numerical frameworks with powerful configurations to simulate multiphase flows. The numerical simulation can be conducted using the finite volume method (FVM) to solve the flow and the heat transfer. Apart from FVM, other methods that are most commonly used are the finite difference method (FDM) and the finite element method (FEM). The FVM is widely used for solving microchannel flow boiling equations due to its inherent conservation properties and ability to handle complex geometries and multiphase flows. However, the choice between FVM, FDM, and FEM ultimately depends on the required specifications of the problem to be solved. The CFD analysis of flow boiling requires a multi-phase computation coupled with a phase-change model to calculate the mass and heat transport across the liquid-vapor interface (Lorenzini & Joshi, 2018).

The primary purpose of this article is to advance the understanding of the finite volume method to solve the governing equations of microchannel flow boiling essential for the development of efficient thermal management solutions for high-performance micro-structured devices. Microchannel flow boiling is a promising cooling technique that leverages phase-change heat transfer to dissipate high

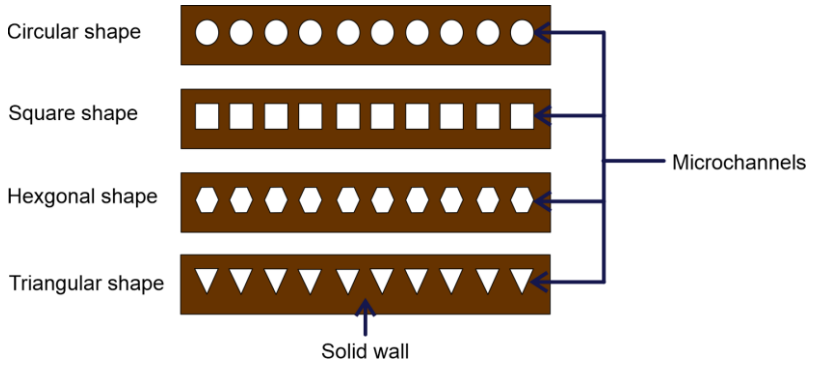

Figure 1. A typical microchannel flow boiling heat-sink with different shapes.

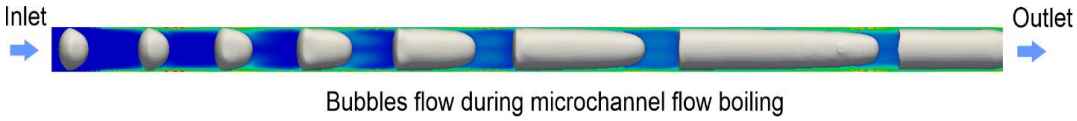

Figure 2. The slug flow pattern of microchannel flow boiling.

heat fluxes in compact systems. The paper contributes to bridging the gap between theoretical models and solution procedures by offering insights into the detailed analysis of microchannel flow boiling cooling technique. In addition, this study is significantly important as it enhances the fundamental understanding of multiphase flow physics required to develop the advanced cooling systems.

NUMERICAL METHOD

The numerical simulation via computational fluid dynamics of microchannel flow boiling requires a computing platform which maybe commercial CFD software or open-source platform to solve the governing equations of the boiling process. The microchannel flow boiling is a two-phase flow (i.e simultaneous flow movement of both liquid and vapour phases) with phase change. As such, the governing equations governing the process comprise the solution of the mass, momentum, energy, and phase-fraction equations.

Governing Equations

The finite volume method is utilized to calculate the conservation equations for the mass, momentum, thermal energy, and phase fraction in the fluid domain. In addition, when the solid wall is taken into account, the conservation equation for the energy is solved as a heat conduction equation. The mass and momentum conservation equations are

$$\frac{\partial(\rho)}{\partial t} + \nabla \cdot (\rho \mathbf{u}) = 0 \qquad (1)$$

$$\frac{\partial(\rho \mathbf{u})}{\partial t} + \nabla \cdot (\rho \mathbf{u}\mathbf{u}) = -\nabla p - \nabla \cdot \{\mu_{\text{eff}}[\nabla \mathbf{u} + (\nabla \mathbf{u})^T]\} + \rho \mathbf{g} + \mathbf{f}_\sigma \qquad (2)$$

where $\mathbf{u}$ is the velocity vector for the two phases (liquid and vapor), ρ and μ_{eff} are the density and the viscosity of the fluid, p is the pressure, and $\mathbf{f}_\sigma$ is the surface tension force (see Eq. (7) in the continuum surface force (CSF) model).

The energy conservation equation is

$$\frac{\partial(\rho c_p T)}{\partial t} + \nabla \cdot (\rho c_p \mathbf{u} T) = \nabla \cdot (k \nabla T) - \dot{q}_{pc} \qquad (3)$$

where T, k, c_p, and $\dot{q}_{pc}$ are the temperature, thermal conductivity, specific heat capacity, and energy changes source term respectively. When the solid wall is considered during the numerical simulation of microchannel flow boiling, the conjugate heat transfer effect is considered and the energy conservation equations for the solid and fluid domains are discretized and solved independently on distinct computational meshes. The temperature and the heat flux continuity conditions are imposed at the solid-fluid interface, while the solid domain's energy

conservation is described by conductive heat transfer equation:

$$\frac{\partial(\rho^s c_p^s T^s)}{\partial t} = \nabla \cdot (k^s \nabla T^s) \tag{4}$$

where T^s, ρ^s, and c_p^s are the microchannel solid wall's temperature, density, and specific heat capacity respectively.

The volume-of-fluid (VOF) method is adopted to simulate the transient liquid-vapor interface dynamics evolving from the phase change phenomena in microchannel flow boiling. The VOF equation is

$$\frac{\partial \alpha}{\partial t} + \nabla \cdot (\mathbf{u}\alpha) = \dot{\alpha}_{pc} \tag{5}$$

where α is the liquid volume-fraction, and $\dot{\alpha}_{pc}$ is the source-term accounting for the phase-change (see the next section). The computational cell represents pure liquid when $\alpha = 1$, it corresponds to pure vapour when $\alpha = 0$, while intermediate values $0 < \alpha < 1$ denotes liquid and vapour mixture. The fluid thermo-physical properties are derived from the volume-fraction

$$\varphi = (1-\alpha)\varphi_v + \alpha\varphi_l \tag{6}$$

where φ denotes any fluid properties, including density, viscosity, and thermal-conductivity.

The influence of surface tension, which is particularly significant for the accurate microchannel flow boiling simulation, is accounted for by introducing an interfacial source term $\mathbf{f}_\sigma$ in Eq. (2) according to Brackbill's continuum surface force (CSF) model (Brackbill et al., 1992). A density multiplier term $2\rho/(\rho_v + \rho_l)$ is applied to the surface tension source term to maintain physical consistency (Brackbill et al., 1992).

$$\mathbf{f}_\sigma = \sigma\kappa\mathbf{n}|\nabla\alpha|\frac{2\rho}{\rho_v + \rho_l} \tag{7}$$

where κ and $\mathbf{n}$ are the curvature and the unit normal vector of the liquid-vapor interface.

$$\kappa = -\nabla \cdot \mathbf{n} \tag{8}$$

$$\mathbf{n} = \frac{\nabla\alpha}{|\nabla\alpha|} \tag{9}$$

Phase change models

Modelling the microchannel flow boiling requires accurate estimation of the mass, momentum, and heat transfer across the liquid-vapour interface. The choice of phase change models is important in predicting the interface evolution during the flow boiling process. Phase change models become complicated due to the need to capture or track the liquid-vapor interface accurately and handle the interfacial mass transfer. Many phase change models are available for solving microchannel flow boiling, however for this study the phase change process at the liquid-vapor interface is modeled using the Hardt and Wondra formulation, while the associated mass transfer is accounted for in the VOF equation (Hardt & Wondra, 2008), and the details can be found in Ref. (Scheufler & Roenby, 2023). The energy source-term, $\dot{q}_{pc}$ in Eq. (3) is evaluated as

$$\dot{q}_{pc} = q_{pc}^l + q_{pc}^v = k^l \nabla T^l \cdot \hat{\mathbf{n}}_s \cdot \frac{A_{\text{int}}}{V} + k^v \nabla T^v \cdot (-\hat{\mathbf{n}}_s) \cdot \frac{A_{\text{int}}}{V} \tag{15}$$

where superscripts *l* and *v* represents liquid and vapour phases respectively, $\hat{\mathbf{n}}_s$ is the interface normal, A_{int} is the interface-surface-area in the cell, and V is the cell-volume. The mass transfer, $\dot{\alpha}_{pc}$ in Eq. (5) is evaluated as

$$\dot{\alpha}_{pc} = \frac{\dot{\rho}}{\rho_l} \tag{16}$$

$$\dot{\rho} = \frac{\dot{q}_{pc}}{h_{lv}} \tag{17}$$

where $\dot{\rho}$ is the volume-specific mass flux at the interface. Eq. (15) is calculated with the normal gradients computed at the liquid-vapour interface.

FINITE VOLUME METHOD (FVM) FRAMEWORK

The numerical simulation is commenced with the generation of a computational mesh by discretizing the solution domain into a number of non-overlapping finite volumes or cells where the conservation equations governing the phenomenon of study are subsequently solved. A typical computational mesh is shown in

Figure 3. The finite volume method (FVM) is a robust numerical technique used to solve the partial differential equations (PDE) governing numerous scientific and engineering field of studies, particularly in computational fluid dynamics (CFD) (Boivin et al., 2000; Saptaningtyas & Setyarsi, 2018). It provides solutions to the PDE by describing the mass, momentum, or energy through a physical domain as a system of algebraic equations. The FVM is characterized by its ability to conserve quantities such as mass, momentum, and energy within control volumes, making it particularly suitable for CFD applications. It also has powerful parallel processing capabilities which can be fully utilized to achieve parallel simulations of microchannel flow boiling. The FVM approach involves the discretization of the integral form of the conservation governing equations over a three-dimensional control volume or computational cell which is a polyhedron. The several stages involved during the discretization process are described in Figure 4.

The FVM discretization procedure can be split into two parts: discretization of time and space. To explain the FVM fundamentals, the governing conservation equations in Eqs. (1) – (3) for the microchannel flow boiling are generalized as one single general transport equation in Eq. (18) to discuss the discretization process over a control volume (CV) for simplicity. The general transport equation (Versteeg & Malalasekra, 2007) for a conserved quantity ϕ is expressed as

$$\frac{\partial \rho\phi}{\partial t} + \nabla\cdot(\rho\mathbf{u}\phi) - \nabla\cdot\left(\rho\Gamma_\phi\nabla\phi\right) = S_\phi(\phi) \qquad (18)$$

where ρ is the density, ϕ is the conserved quantity (e.g., mass, momentum, energy), $\mathbf{u}$ is the velocity vector, Γ_ϕ is the diffusion coefficient, and S_ϕ is the source term. The three terms at the left hand side of the general transport equation are called the temporal derivative, convective term, and diffusion term respectively (Ferziger et al., 2019; Patankar, 2018). For instance, by defining the variables in Eq. (18) to

$$\phi = 1, \quad \Gamma_\phi = 0, \quad S_\phi = 0$$

The transport equation becomes the mass conservation equation in Eq. (1) as

$$\frac{\partial(\rho)}{\partial t} + \nabla\cdot(\rho\mathbf{u}) = 0$$

Hence, by defining the variables ϕ, Γ_ϕ, and S_ϕ in Eq. (18) with the corresponding momentum and energy terms in the conservation equations will lead to the Eqs. (2) and (3). The general transport equation (Eq. (2)-(18)) is a second order equation, as such the FVM discretization order must be equal or greater than the order of the equation to achieve good accuracy. Figure 5 shows a control volume in which the PDE is discretized. The control volume comprises a set of faces bounded together with only one face connected to a particular neighbour CV face. It has a centroid with a point *P* for the computation.

The transport equation integral over the finite control-volume is

$$\int_{V_P}\frac{\partial\rho\phi}{\partial t}dV + \int_{V_P}\nabla\cdot(\rho\mathbf{u}\phi)dV - \int_{V_P}\nabla\cdot\left(\rho\Gamma_\phi\nabla\phi\right)dV = \int_{V_P}S_\phi(\phi)dV \qquad (19)$$

where *V* is the volume. After completing the integration over the CV, the Gauss or Divergence theorem is applied to convert the volume integrals of the convection and diffusion terms into surface integrals. The Gauss theorem states that the volume integral of the divergence of a vector field is equal to the surface integral of that field over the boundary of that volume. Mathematically, for a given general vector field *F* defined over a control volume *V* as shown in Figure 6 with a closed surface boundary *S*, the theorem is defined as

$$\int_{V_P}\nabla\cdot F\,dV = \oiint_{\partial V_P} F\cdot\mathbf{n}\,dS = \oiint_{\partial V_P} d\mathbf{S}\cdot F \qquad (20)$$

where $\mathbf{n}$ is the unit outward normal vector to the surface *S*, and $\mathbf{n}dS = d\mathbf{S}$.

Therefore, Eq. (19) is written with Gauss theorem in Eq. (21) and the discretisation is subsequently done term by term because the equation is commutative.

$$\frac{\partial}{\partial t}\int_{V_P}(\rho\phi)dV + \oiint_{\partial V_P} d\mathbf{S}\cdot(\rho\mathbf{u}\phi) - \oiint_{\partial V_P} d\mathbf{S}\cdot\left(\rho\Gamma_\phi\nabla\phi\right) = \int_{V_P}S_\phi(\phi)dV \qquad (21)$$

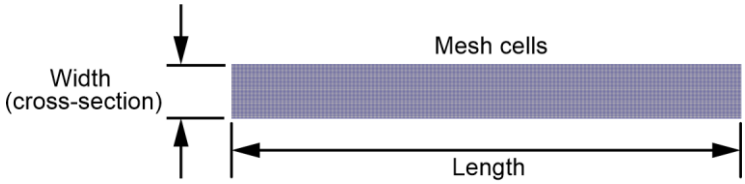

Figure 3. A typical computational highly refined mesh.

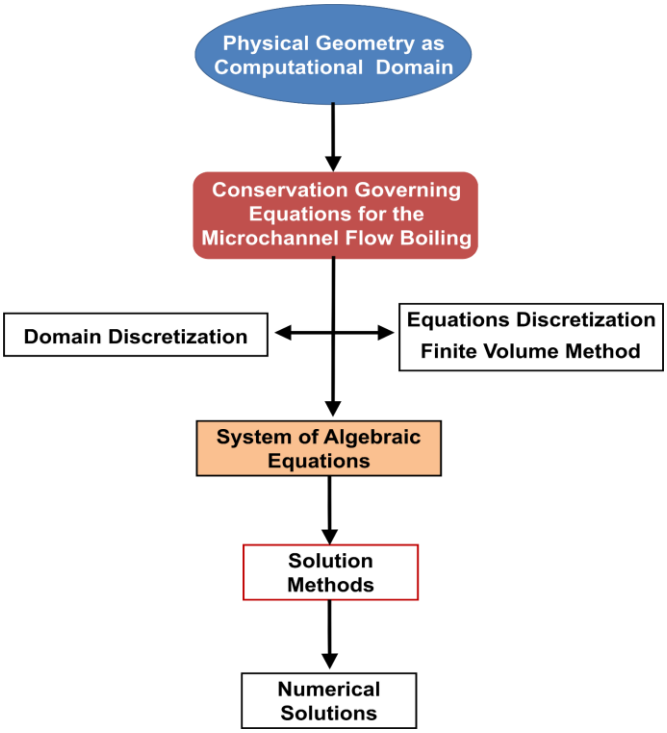

Figure 4. The stages of the discretization process.

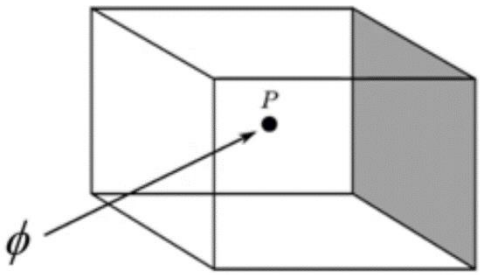

Figure 5. Control volume.

By integrating each term in space, the convection term becomes

$$\int_{V_P} \nabla\cdot(\rho\mathbf{u}\phi)dV = \oint_{\partial V_P} d\mathbf{S}\cdot(\rho\mathbf{u}\phi) = \sum_f \int_f d\mathbf{S}\cdot(\rho\mathbf{u}\phi)_f \tag{22}$$

$$\approx \sum_f \mathbf{S}_f \cdot \left(\overline{\rho\mathbf{u}\phi}\right)_f = \sum_f \mathbf{S}_f \cdot (\rho\mathbf{u}\phi)_f \tag{23}$$

where subscript *f* is the middle face value of the variable of the CV. The integrant is approximated at the mid-point, which is second order accurate. The diffusion term becomes

$$\int_{V_P} \nabla\cdot\left(\rho\Gamma_\phi\nabla\phi\right)dV = \oint_{\partial V_P} d\mathbf{S}\cdot\left(\rho\Gamma_\phi\nabla\phi\right) = \sum_f \int_f d\mathbf{S}\cdot\left(\rho\Gamma_\phi\nabla\phi\right)_f \tag{24}$$

$$\approx \sum_f \mathbf{S}_f \cdot\left(\overline{\rho\Gamma_\phi\nabla\phi}\right)_f = \sum_f \mathbf{S}_f \cdot\left(\rho\Gamma_\phi\nabla\phi\right)_f \tag{25}$$

And for a linear source term, it is approximated as

$$\int_{V_P} S_\phi(\phi)dV = S_c V_P + S_P V_P \phi_P \tag{26}$$

where S_c and S_p are the constant part and non-linear part of the source terms respectively. In the treatment of the second order FVM, the variable ϕ is stored at the cell centroid and assumed to vary linearly across the cells (Mu & Ye, 2011; Saptaningtyas & Setyarsi, 2018). The FVM discretization interpolation is done by considering both the owner cell with centroid point *P* and the neighbour cell with centroid point *N* as shown in Figure 7. The number of the neighbour cells depends on the number of sides of the owner cell. Eqs. (23) and (25) require the differencing schemes to calculate the face value of the variable ϕ from the cell centres values.

After the spatial discretisation of the equation terms, the general transport equation in Eq. (19) can be written in semi-discrete equation as

$$\int_{V_P} \frac{\partial\rho\phi}{\partial t}dV + \sum_f \mathbf{S}_f\cdot(\rho\mathbf{u}\phi)_f - \sum_f \mathbf{S}_f\cdot\left(\rho\Gamma_\phi\nabla\phi\right)_f = \left(S_c V_P + S_P V_P \phi_P\right) \tag{27}$$

The temporal discretization can be determined from Eq. (27) as

$$\int_t^{t+\Delta t}\left[\left(\frac{\partial\rho\phi}{\partial t}\right)_P V_P + \sum_f \mathbf{S}_f\cdot(\rho\mathbf{u}\phi)_f - \sum_f \mathbf{S}_f\cdot\left(\rho\Gamma_\phi\nabla\phi\right)_f\right]dt = \int_t^{t+\Delta t}\left(S_c V_P + S_P V_P\phi_P\right)dt \tag{28}$$

Within the temporal discretization process, any time discretization scheme can be applied (*e.g.*, Crank-Nicolson, backward differencing, Euler implicit, forward Euler, etc.) and each term in Eq. (28) can be treated differently to achieve good accuracies, so far the individual terms are calculated to be at least second order accurate.

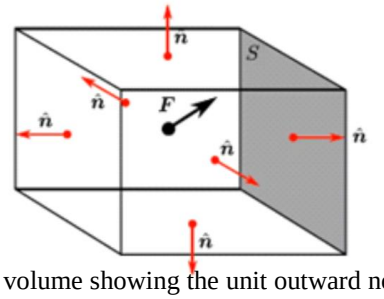

Figure 6. Control volume showing the unit outward normal vector to the surfaces.

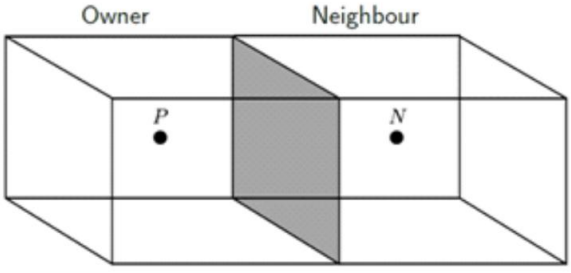

Figure 7. The owner and neighbour cells.

SOLUTION PROCEDURES

The numerical simulation of microchannel flow boiling using either a commercial CFD software (e.g ANSYS, COMSOL) or open-source platform (e.g OpenFOAM) is a complex process that involves several procedures to be carried out in order to achieve accurate and reliable results. In this section, the solution procedures are outlined.

1. The first step in the simulation process is to set up the physical geometry of the microchannel as the computational domain and define the boundary conditions. In this step, a design model of the microchannel will be carried out with a computer aided design (CAD) application tools. This includes specifying the dimensions of the microchannel.
2. Secondly, the designed model of the physical geometry is discretized into finite grid or mesh sizes. The discretization of the domain into mesh cells must be sufficiently and highly refined in the fluid region where the boiling process occurs and near the walls or in the vicinity of vapor bubbles. This is important to achieve accurate simulation results.
3. Subsequently, the specification of the initial boundary conditions for the inlet, outlet, walls, and any other relevant surfaces are carried out on the discretized domain. This includes specifying pressure, velocity, temperature, phase fractions, and wall temperatures for the flow boiling simulation.
4. Then the simulation begins with the solver solving the governing equations of the mass, momentum, energy, and phase fraction equations (Eqs. (1) – (4)) in the microchannel domain and computes the flow fields over time. In this step, the numerical discretization of the governing equations is done by converting the continuous partial differential equations into a system of algebraic equations by using the finite volume method (FVM) as shown from Eq. (22) upwards. The FVM integrates the governing equations over control volumes, ensuring conservation properties (Versteeg & Malalasekera, 2007). The discretization involves the approximation of the spatial and temporal derivatives with schemes such as upwind, central differencing, or high-order methods chosen based on stability and accuracy requirements. Further, the discretized system of algebraic equations is solved using numerical solvers. The solver selection depends on the problem type, mesh size, and computational resources available.
5. To determine a computationally efficient yet accurate discretization scheme, a grid convergence analysis is performed to verify that the selected mesh resolution sufficiently resolves the evolving vapor-liquid interface during microchannel bubble growth and validation is also done in order to verify the accuracy of the model, where the numerical results are analyzed and compared with experimental or analytical data.
6. Finally, after completing the simulations, the results are post-processed to analyze the flow boiling behavior in the microchannel. This includes visualizing the flow and temperature fields, evaluating the vapor bubbles growth and convective heat transfer, and also by extracting other quantities of research interests. The post-processing also includes the visualization of the flow fields in terms of the velocity contours and streamlines, and the pressure distribution.

CONCLUSION

The finite volume method provides a robust framework for simulating microchannel flow boiling by discretizing the governing equations into algebraic forms and solving them iteratively. The finite volume method provides a powerful framework for solving the governing equations of microchannel flow boiling, capturing the intricate interplay of fluid dynamics, heat transfer, and phase change. By discretizing the domain into control volumes and employing robust numerical schemes, FVM ensures conservation and accuracy. The solution procedure involves iterative coupling of the continuity, momentum, energy, and VOF equations, with careful treatment of phase-change and interfacial effects. Despite challenges like numerical stability and computational cost, FVM remains a

cornerstone of computational fluid dynamics for advanced cooling technologies, enabling detailed insights into microchannel flow boiling performance. This approach is critical for the understanding of microchannel heat sinks in high-performance cooling applications.

REFERENCES

Al-Zaidi, A. H., Mahmoud, M. M., & Karayiannis, T. G. (2019). Flow boiling of HFE-7100 in microchannels: Experimental study and comparison with correlations. *International Journal of Heat and Mass Transfer, 140*, 100-128. https://doi.org/10.1016/j.ijheatmasstransfer.2019.05.095

Boivin, S., Cayré, F., & Hérard, J.-M. (2000, 2000/09/01/). A finite volume method to solve the Navier–Stokes equations for incompressible flows on unstructured meshes. *International Journal of Thermal Sciences, 39*(8), 806-825. https://doi.org/https://doi.org/10.1016/S1290-0729(00)00276-3

Brackbill, J. U., Kothe, D. B., & Zemach, C. (1992). A continuum method for modeling surface tension. *Journal of Computational Physics, 100*(2), 335-354. https://doi.org/10.1016/0021-9991(92)90240-y

Ferrari, A., Magnini, M., & Thome, J. R. (2018, Aug). Numerical analysis of slug flow boiling in square microchannels. *International Journal of Heat and Mass Transfer, 123*, 928-944. https://doi.org/10.1016/j.ijheatmasstransfer.2018.03.012

Ferziger, J. H., Perić, M., & Street, R. L. (2019). *Computational methods for fluid dynamics*. springer.

Hardt, S., & Wondra, F. (2008, May). Evaporation model for interfacial flows based on a continuum-field representation of the source terms [Article]. *Journal of Computational Physics, 227*(11), 5871-5895. https://doi.org/10.1016/j.jcp.2008.02.020

Harirchian, T., & Garimella, S. V. (2010, 2010/06/01/). A comprehensive flow regime map for microchannel flow boiling with quantitative transition criteria. *International Journal of Heat and Mass Transfer, 53*(13), 2694-2702. https://doi.org/https://doi.org/10.1016/j.ijheatmasstransfer.2010.02.039

Harirchian, T., & Garimella, S. V. (2011). Boiling heat transfer and flow regimes in microchannels—A comprehensive understanding. *Journal of Electronic Packaging, 133*(1), 011001. https://doi.org/10.1115/1.4002721

Harirchian, T., & Garimella, S. V. (2012, 2012/01/31/). Flow regime-based modeling of heat transfer and pressure drop in microchannel flow boiling. *International Journal of Heat and Mass Transfer, 55*(4), 1246-1260. https://doi.org/10.1016/j.ijheatmasstransfer.2011.09.024

Jain, S., & Gedupudi, S. (2020, 2020/11/29). On the prediction of pressure fluctuations and pressure drop caused by confined bubble growth during flow boiling in a rectangular mini/micro-channel. *Heat Transfer Engineering, 41*(21), 1763-1783. https://doi.org/10.1080/01457632.2019.1670456

Karayiannis, T. G., & Mahmoud, M. M. (2017, 2017/03/25/). Flow boiling in microchannels: Fundamentals and applications. *Applied Thermal Engineering, 115*, 1372-1397. https://doi.org/https://doi.org/10.1016/j.applthermaleng.2016.08.063

Lorenzini, D., & Joshi, Y. K. (2018). Computational fluid dynamics modeling of flow boiling in microchannels with nonuniform heat flux. *Journal of Heat Transfer, 140*(1), 011501. https://doi.org/10.1115/1.4037343

Magnini, M., & Matar, O. K. (2020). Numerical study of the impact of the channel shape on microchannel boiling heat

transfer. *International Journal of Heat and Mass Transfer, 150*, 119322. https://doi.org/10.1016/j.ijheatmasstransfer.2020.119322

Mu, L., & Ye, X. (2011, 2011/12/01/). A finite volume method for solving Navier–Stokes problems. *Nonlinear Analysis: Theory, Methods & Applications, 74*(17), 6686-6695. https://doi.org/https://doi.org/10.1016/j.na.2011.06.048

Mudawar, I. (2011). Two-Phase Microchannel Heat Sinks: Theory, Applications, and Limitations. *Journal of Electronic Packaging, 133*(4). https://doi.org/10.1115/1.4005300

Mudawar, I. (2013). Recent advances in high-flux, two-phase thermal management. *Journal of Thermal Science and Engineering Applications, 5*(2), 021012. https://doi.org/10.1115/1.4023599

Odumosu, O. A., Li, H., Wang, T., & Che, Z. (2024). Conjugate heat transfer effects on bubble growth during flow boiling heat transfer in microchannels. *Physics of Fluids, 36*(12), 122110. https://doi.org/10.1063/5.0242693

Odumosu, O. A., Xu, H., Wang, T., & Che, Z. (2023). Growth of elongated vapor bubbles during flow boiling heat transfer in wavy microchannels. *Applied Thermal Engineering, 223*, 119987. https://doi.org/https://doi.org/10.1016/j.applthermaleng.2023.119987

Patankar, S. (2018). *Numerical heat transfer and fluid flow*. CRC press.

Prakash, S., & Kumar, S. (2014, 2015/08/01). Fabrication of microchannels: A review. *Proceedings of the Institution of Mechanical Engineers, Part B: Journal of Engineering Manufacture, 229*(8), 1273-1288. https://doi.org/10.1177/0954405414535581

Qu, W., Yoon, S.-M., & Mudawar, I. (2004). Two-phase flow and heat transfer in rectangular micro-channels. *Journal of Electronic Packaging, 126*(3), 288-300. https://doi.org/10.1115/1.1756589

Revellin, R., Dupont, V., Ursenbacher, T., Thome, J. R., & Zun, I. (2006, 2006/07/01/). Characterization of diabatic two-phase flows in microchannels: Flow parameter results for R-134a in a 0.5mm channel. *International Journal of Multiphase Flow, 32*(7), 755-774. https://doi.org/10.1016/j.ijmultiphaseflow.2006.02.016

Saha, K. S., Piero Celata, G., & Kandlikar, S. G. (2011). Thermofluid dynamics of boiling in microchannels. In Y. I. Cho & G. A. Greene (Eds.), *Advances in Heat Transfer* (Vol. 43, pp. 77-226). Elsevier. https://doi.org/https://doi.org/10.1016/B978-0-12-381529-3.00002-5

Saptaningtyas, F. Y., & Setyarsi, A. D. (2018, 2018/09/01). Finite Volume Method with Explicit Scheme Technique for Solving Heat Equation. *Journal of Physics: Conference Series, 1097*(1), 012089. https://doi.org/10.1088/1742-6596/1097/1/012089

Scheufler, H., & Roenby, J. (2023, 12/02). TwoPhaseFlow: A framework for developing two phase flow solvers in OpenFOAM. *OpenFOAM® Journal, 3*, 200-224. https://doi.org/10.51560/ofj.v3.80

Thome, J. R., & Cioncolini, A. (2015). Two-phase flow pattern maps for microchannels. In *Encyclopedia of two-phase heat transfer and flow I* (pp. 47-84). World Scientific. https://doi.org/doi:10.1142/9789814623216_0020

Versteeg, H., & Malalasekra, W. (2007). *An introduction to computational fluid dynamics: The finite volume method* (2ed ed.). Pearson, Harlow.